IOPscience iopscience.iop.org

Home Search Collections Journals About Contact us My IOPscience

Adsorbing bargraph paths in a *q*-wedge

This article has been downloaded from IOPscience. Please scroll down to see the full text article.

2005 J. Phys. A: Math. Gen. 38 8505

(http://iopscience.iop.org/0305-4470/38/40/003)

View the table of contents for this issue, or go to the journal homepage for more

Download details:
IP Address: 171.66.16.94
The article was downloaded on 03/06/2010 at 03:59

Please note that terms and conditions apply.

INSTITUTE OF PHYSICS PUBLISHING JOURNAL OF PHYSICS A: MATHEMATICAL AND GENERAL

J. Phys. A: Math. Gen. **38** (2005) 8505–8525 doi:10.1088/0305-4470/38/40/003

Adsorbing bargraph paths in a q-wedge

E J Janse van Rensburg

Department of Mathematics and Statistics, York University, 4700 Keele Street, Toronto, Ontario, M3J 1P3, Canada

E-mail: rensburg@yorku.ca

Received 16 June 2005, in final form 23 August 2005
Published 21 September 2005
Online at stacks.iop.org/JPhysA/38/8505

Abstract
Consider a model of partially directed paths from the origin in the square lattice, constrained to the region between the Y-axis and the line $Y = qX$, and ending in a vertex in this line (with coordinates of the form (N, Nq), and where $q > 0$ is an integer). Such paths are bargraph paths in a q-wedge. In this paper the adsorption of bargraph paths in the line $Y = qX$ is examined. This model has generating function $g_q(t, z)$ where t is the edge generating variable and z is the generating variable of visits of the path to the line $Y = qX$. It is proven that the model undergoes an adsorption transition at the critical value of z_q and that z_q is given asymptotically by

$$z_q = \frac{3q + 4 + \log q - \sqrt{\log^2 q + \log q^2 + 4}}{4 + \log q - \sqrt{\log^2 q + \log q^2 + 4}} + O\left(\frac{q}{|\log q|^3}\right).$$

In other words, z_q/q is given to decaying terms. Moreover, adsorbing bargraph paths in a $1/p$-wedge between the Y-axis and the line $Y = (1/p)X$, where $p > 0$ is an integer, are also considered. In these models it is shown that $z_{1/p} \simeq p^2/2 \log p^2$ for large p.

PACS numbers: 05.50.+q, 02.10.Ab, 05.40.Fb, 82.35.−x

1. Introduction

Directed and partially directed lattice paths have been used for some decades as simple lattice models of polymers. These models are simplification of the self-avoiding walk, which is the most natural lattice model of a polymer [11, 23]. The self-avoiding walk is non-Markovian, and although many of its properties are now known or have been estimated, it remains a challenging model, especially in three dimensions; see for example [17]. Recent developments in Schramm–Loewner excursions (SLE) and conformal invariance have apparently advanced the understanding of this model in two dimensions [16]. In five and higher dimensions,

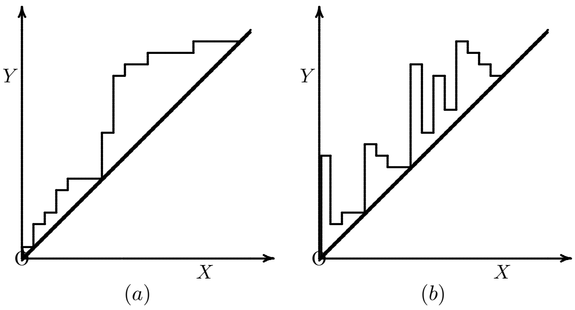

Figure 1. (*a*) A directed path confined to a wedge. (*b*) A partially directed path in a wedge. If the path is constrained to end in the diagonal line, then this is a bargraph path confined to a wedge.

the lace expansion has been used to show that self-avoiding walks have a Gaussian scaling limit [13].

Models of self-avoiding walks confined to wedges have been studied as a model of a polymer in a wedge geometry [6, 9, 12], and this model has been approached using conformal invariance [5]. There are also results for self-avoiding walks in the vicinity of an excluded needle [4]. Branched polymers [7, 8, 10] and polymer networks [1, 24] have also been studied in wedge geometries, and their critical exponents have been determined.

The literature on directed models in confined geometries are sporadic. Directed percolation and directed animals have been considered in wedge geometries [25], and fully directed paths have been studied recently in a slit geometry [3].

Directed and partially directed paths, in contrast to the self-avoiding walk, are better understood, and in some cases have been solved exactly. Nevertheless, the models do retain some of the features and qualities of the self-avoiding walk, and so are a useful laboratory for examining the properties of models of linear polymers. In this paper, the focus will in particular be on paths in wedges as a model of a polymer chain in a restricted geometry in two dimensions.

Fully directed paths in a wedge geometry were examined in [14], and the forces that such a path exerts when squeezed in a wedge were examined in [15]. In this paper, some of the techniques in those papers are applied to the more general model of partially directed paths confined to a wedge. We will in particular focus on a model of *bargraph paths* in a wedge; this is a model of partially directed paths in a wedge geometry counted by length and interacting with the boundary of the wedge, see figure 1. Bargraph paths are closely related to bargraph polygons [21], which are also a model of a directed vesicle near a wall [2]. The results in this paper generalize in particular the model in [22] to a certain class of wedge geometries.

In section 2 a model of adsorbing bargraph paths is defined. This is a model of partially directed paths from the origin in the positive half-plane, but with terminal vertex in the X-axis. A model of adsorbing bargraph paths is defined by the generating function

$$g_b(t,z) = g_{b,z} = \sum_{n>0} \left[\sum_{v \geqslant 0} b_n(v) z^v \right] t^n, \tag{1}$$

where $b_n(v)$ is the number of bargraph paths of length n and with v vertices (visits) in the X-axis. The generating function $g_{b,z}$ can be determined in closed form and the critical values of the edge generating variable t and the visit generating variable z are known: $t_b = \sqrt{2} - 1$ and $z_b = (\sqrt{5} - 1)/2(\sqrt{2} - 1)$.

In section 3 the results in section 2 are revisited, but using an approach developed for directed paths in [14]. This enables one to determine critical points without explicitly solving for the generating function. This will be a useful technique in analysing bargraph paths in wedges where one apparently cannot determine the generating function in closed form.

Bargraph paths in a wedge defined by the Y-axis and the line $Y = X$ are examined in section 4. More generally, a model of bargraphs in a q-wedge formed by the Y-axis and the line $Y = qX$, where q is a non-negative integer, is defined. A recurrence relation is determined for the case $q = 1$, and the critical value of the visit generating variable z is determined to be $z_1 = 5/2$.

The full model for general q is examined in section 5. Functional recurrences are determined to enumerate bargraph paths in q-wedges (these are q-bargraph paths), and I analyse these to determine the critical value of t; this is the radius of convergence of the generating function of q-bargraph paths (when $z = 1$). I derive in particular a set of equations (see equations (50)–(53)) which may be solved to give t_q (the critical value of t) as well as $g_q^* = g_q(t_q)$; this is the value of the generating function at the critical point. This turns out to be finite, similar to the situation observed for Dyck paths in q-wedges (see [14]). The adsorption critical point z_q can be determined from these results, and by solving numerically one may determine the critical point in this model. This is shown in table 2. Next, an asymptotic formula is developed for adsorbing q-bargraph paths: the critical point is given by

$$z_q = \frac{3q + 4 + \log q - \sqrt{\log^2 q + \log q^2 + 4}}{4 + \log q - \sqrt{\log^2 q + \log q^2 + 4}} + O\left(\frac{q}{|\log q|^3}\right). \tag{2}$$

This approximation turns out to be very accurate, even for moderate values of q.

In section 7 the adsorption of bargraph paths in $1/p$-wedges, where $p > 0$ is an integer, is examined. Similar to the case for q-wedges, a set of functional recurrences is determined from which the critical point can be determined. Solving numerically gave the values in table 3. The critical point can also be approximated, and it is shown that

$$z_{1/p} = 1 + (1 + o(1))\left[\frac{p(p+1)/2}{1 + \log(p(p+1)/2)}\right]\exp\left(\frac{\log(1 + \log(p(p+1)/2))}{1 + \log(p(p+1)/2)}\right). \tag{3}$$

This approximation, while increasingly good for increasing values of p, is not of the same quality as the estimate in equation (2).

2. Adsorbing bargraph paths

A *partially directed path* from the origin of the square lattice is a path constrained to step from the origin by giving steps only in the East, North or South directions, and which cannot make a South step immediately after a North step, or vice versa. The path never steps West, and it traces a self-avoiding path with horizontal edges oriented in the East direction. In figure 2(a) an example of a partially directed path is given. In this example, the path does not visit sites below the X-axis, but it may do so. If a partially directed path is constrained (1) to have its terminal vertex in the X-axis, and (2) not to step below the X-axis, then it is a *bargraph path* (or a *bargraph polygon* if it is enumerated by total perimeter length and enclosed area). An example of a bargraph path is given in figure 2(b). A bargraph path encloses the area in the square lattice between the X-axis and itself, and bargraph polygons have been used as lattice models of vesicles [2].

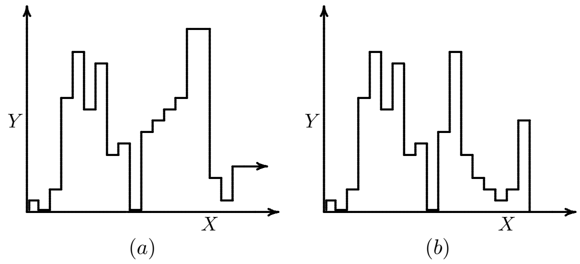

Figure 2. (*a*) A partially directed path. (*b*) A bargraph path.

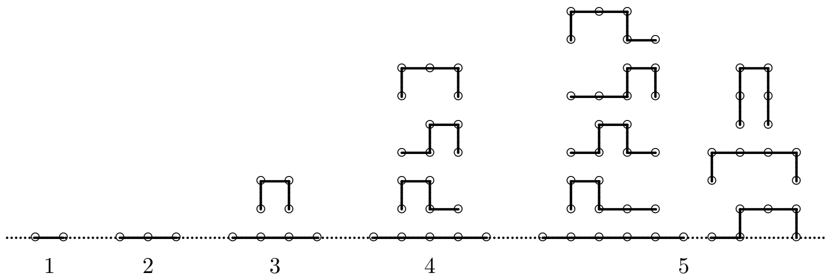

Figure 3. Bargraph paths enumerated to length 5 edges. The numbers of these paths are listed in table 1.

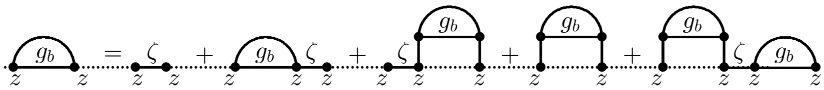

Figure 4. Every bargraph path is either a single horizontal edge, or it is an arbitrary bargraph path ending in a horizontal edge, or it is a horizontal edge followed by a primitive bargraph path, or it is a primitive bargraph path, or it is a primitive bargraph path, followed by a horizontal edge and then followed by an arbitrary bargraph path; see [20]. Two models of adsorbing bargraph paths can be defined: either the vertices adsorb in the X-axis with activity or generating variable z, or the edges adsorb in the X-axis with activity or generating variable ζ. The resulting functional recursions for the generating functions are given by equations (6) or (7).

The first few bargraph paths are illustrated in figure 3. Let the number of such bargraph paths of length n be b_n. Then $b_1 = 1,\ b_2 = 1,\ b_3 = 2b_4 = 4,\ b_5 = 8,\ b_6 = 16, \ldots,$ $b_{40} = 15\,499\,732\,274\,689$. The generating function

$$g_b(t) := \sum_{n=0}^{\infty} b_n t^n \tag{4}$$

of bargraphs paths is known [20], and it can be determined by solving a functional recurrence. The generating variable of edges is t, and I shall often suppress it by putting $g_b \equiv g_b(t)$.

A bargraph path is *primitive* if it has only its first and last vertices in the X-axis, but otherwise contains only vertices with strictly positive Y-coordinate. By considering primitive bargraphs paths, and primitive parts of bargraph paths, a recurrence can be determined for the generating function g_b.

Observe that every bargraph path can be classified to belong to one of the five classes. That is, every bargraph path is either (1) the single edge as in figure 4, or (2) it ends in a horizontal edge, or (3) its first edge is horizontal, but it is primitive after this edge, or (4) it is primitive (its first and last edges are vertical), or (5) it is primitive and returns a first time to the X-axis (where it must step horizontally), before it continues as an arbitrary bargraph path. These classes are illustrated in figure 4.

Ignore the labels z and ζ in figure 4. The generating function g_b is indicated by semicircular bubbles and edges joining these together in the five classes are drawn. Noting that edges are generating by t enables one to write a recurrence for g_b:

$$g_b = t + tg_b + t^3 g_b + t^2 g_b + t^3 g_b^2. \tag{5}$$

This recurrence is quadratic in g_b; one of the roots will give the generating function of bargraph paths, with t counting the number of edges in the path.

In a model of *adsorbing bargraph paths* the number of vertices, or the number of edges, of the path in the X-axis is also tracked. There are two models of adsorbing bargraph paths. The first is a model of *vertex-adsorbing bargraphs*. A *visit* is vertex of the path in the X-axis, and I assign the generating variable z to such visits in figure 4. By repeating the above arguments, and tracking visits, the generating function $g_{b,z}$ in equation (1) of adsorbing bargraphs in the visit-length ensemble satisfies the recurrence

$$g_{b,z} = tz^2 + tzg_{b,z} + t^3 z^3 g_{b,1} + t^2 z^2 g_{b,1} + t^3 z^2 g_{b,1} g_{b,z}. \tag{6}$$

Observe the notation in this equation: I indicate the visit generating variable z by appending it as a subscript to $g_{b,z}$. The generating function $g_{b,1} = g_b$ is the solution of equation (5) when $z = 1$.

The second model is obtained when edges of the path in the X-axis are tracked; these are *edge visits*, and they will be generated by ζ. The techniques here show that the generating function $g_{b,\zeta}$ of adsorbing bargraph paths in the edge-visit ensemble satisfies the recurrence

$$g_{b,\zeta} = t\zeta + t\zeta g_{b,\zeta} + t^3 \zeta g_{b,1} + t^2 g_{b,1} + t^3 \zeta g_{b,1} g_{b,\zeta}. \tag{7}$$

One may combine these models in a single adsorbing bargraph path with generating function $g_{b,z,\zeta}$ satisfying the recurrence

$$g_{b,z,\zeta} = tz^2\zeta + tz\zeta g_{b,z,\zeta} + t^3 z^3 \zeta g_{b,1,1} + t^2 z^2 g_{b,1,1} + t^3 z^2 \zeta g_{b,1,1} g_{b,z,\zeta}. \tag{8}$$

The solutions of the recurrences can be determined by first solving equation (5): the root with non-negative coefficients is

$$g_b = \frac{1 - t - t^2 - t^3 - \sqrt{(1 - t^4)(1 - 2t - t^2)}}{2t^3}. \tag{9}$$

The radius of convergence of this generating function is given by a branch point when $1 - 2t - 2t^2 = 0$. This shows that $t_b = \sqrt{2} - 1$, and t_b is the *critical value* of the generating variable t. It also follows that $g_b(t_b) = 1 + \sqrt{2}$.

It is now possible to solve for $g_{b,z}$, $g_{b,\zeta}$ and $g_{b,z,\zeta}$ in terms of g_b in equation (9). The resulting expressions are somewhat complicated and are given by

$$g_{b,z} = \frac{tz^2 + t^2 z^2 (tz + 1) g_{b,1}}{1 - tz(1 + t^2 z g_{b,1})}; \tag{10}$$

$$g_{b,\zeta} = \frac{t\zeta + t^2 (t\zeta + 1) g_{b,1}}{1 - t\zeta - t^3 \zeta g_{b,1}}; \tag{11}$$

$$g_{b,z,\zeta} = \frac{tz^2\zeta + t^2 z^2 (tz\zeta + 1) g_{b,1,1}}{1 - tz\zeta - t^3 z^2 \zeta g_{b,1,1}}. \tag{12}$$

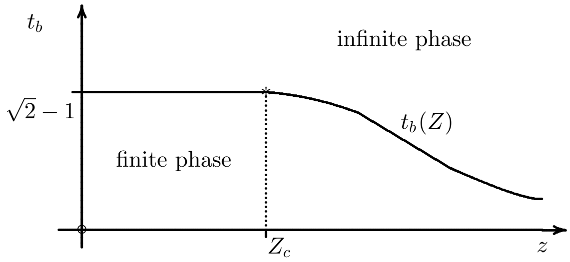

Figure 5. The radius of convergence of the generating functions $g_{b,z}$ or for $g_{b,\zeta}$, where Z denoted either z or ζ. For small values of Z, t_b is determined by a branch point when the radical vanishes in the generating function: this shows that $t_b = \sqrt{2}-1$ when Z is small. Increasing Z will give a regime where t_b is determined by a simple pole in g_b; the changeover occurs at a value $Z = z_b$ in the model of vertex-adsorbing bargraph paths and for $Z = \zeta_b$ in the model of edge-adsorbing bargraph paths. The curve g_b is non-analytic at this point, and in the thermodynamic picture signals a phase transition. In these models the critical points are $z_b = (\sqrt{5}-1)/2(\sqrt{2}-1)$ and $\zeta_b = 1 + 1/\sqrt{2}$ respectively.

The radius of convergence of these generating functions can be determined by noting that there is a curve of simple poles when the denominator vanishes. For example, in the case of $g_{b,z}$ this is given by

$$t_{b,z} = \min\{t | t = \sqrt{2}-1, tz(1+t^2 z g_{b,1}) = 1\}. \tag{13}$$

A generic plot of the radius of convergence is given in figure 5.

The free energy in this model is given by $\mathcal{F}_b(z) = -\log t_{b,z}$. $\mathcal{F}_b(z)$ is a constant for small values of z ($\mathcal{F}_b(z) = \log(1+\sqrt{2}) = -\log t_b$), but it becomes dependent on z at the solution of

$$t_b z\left(1 + t_b^2 z g_{b,1}\right) = 1, \tag{14}$$

since this value of z is obtained when the two functions in the minimum in equation (13) are equal. In other words, if $z = z_b$ is the solution of equation (13), then the point (z_b, t_b) in the critical curve of this model separates the radius of convergence $t_{b,z}$ into a part determined by the branch point in the radical in the generating function $g_{b,1}$, and a part determined by a simple pole when the denominator in equation (10) vanishes.

Solving for z in equation (14) gives the critical point

$$z_b = \frac{\sqrt{5}-1}{2(\sqrt{2}-1)} = 1.492\,066\ldots. \tag{15}$$

The critical point can similarly be determined in the edge adsorption model. In particular, the critical value of ζ is in that case

$$\zeta_b = 1 + \tfrac{1}{\sqrt{2}} = 1.707\,106\ldots. \tag{16}$$

The general model which includes both a vertex generating variable z and an edge generating variable ζ also exhibits a critical curve and an adsorption transition. In this case the model may be analysed in the $z\zeta$-plane, and there is a critical curve of adsorption transitions given by

$$\zeta z(z(3-\sqrt{8}) + \sqrt{2} - 1) = 1. \tag{17}$$

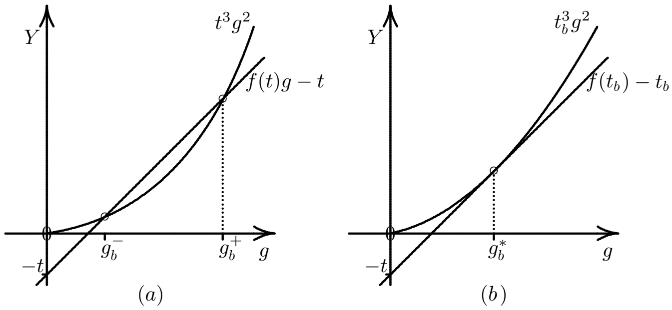

Figure 6. A plot of the curves in equation (19), where $f(t) = 1-t-t^2-t^3$. (*a*) The intersections between these curves give solutions of the recurrence in equation (5) or in equation (18). If t is increased to t_b, then the curves will intersect in exactly one value of $g > 0$. By determining the coordinates of this intersection, both t_b and $g_b(t_b) = g_b^*$ can be determined. This gives both the radius of convergence of g_b, and its value at this value of t.

3. Determining the critical point in adsorbing bargraph paths

In section 2, the critical values of z and ζ were determined by solving for the generating function of bargraphs. In this section, I will briefly review the determination of the critical points from a different point of view; this was first done for adsorbing directed paths in [14]. Consider first a model of adsorbing partially directed paths with a vertex generating variable z. The generating function of this model is given by equation (10), and it satisfies the recurrence in equation (6).

To solve for the critical point z_b, the full generating function was determined in the previous section, and from it the value of z_b was determined. A simpler approach can be followed. The starting point is the recurrence in equation (5). Put this recurrence into the form

$$t^3 g_b^2 = (1-t-t^2-t^3)g_b - t. \tag{18}$$

For fixed values of t, the solutions to this polynomial in g_b are given by the intersection of a parabola with a line in the Yg-plane, given by

$$Y = t^3 g^2, \qquad Y = (1-t-t^2-t^3)g - t. \tag{19}$$

These curves are plotted in figure 6. In figure 6(*a*) t is sufficiently small that there are two points of intersection $g = g_b^{\pm}$ between the graphs. An examination of the solution shows that g_b^- is the root that enumerates partially directed paths. The radius of convergence t_b of g_b in equation (9) can be determined by considering figure 6(*b*). In this case t has increased to t_b, where there are exactly one solution with $g_b > 0$. For $t > t_b$ there are no positive solutions, so t_b is the radius of convergence of g_b. Define $g_b^* = g_b(t_b)$. The value of t_b and g_b^* can be determined by determining the coordinates of the intersection between the two curves.

To determine the point of intersection in figure 6(*b*), note that the line $Y = (1-t-t^2-t^3)g - t$ is tangent to the curve $Y = t^3g^2$ at the point $(g_b^*, Y(g_b^*))$ with $t = t_b$. This tangent has formula

$$Y = 2t_b^3 g_b^* g - t_b^3 [g_b^*]^2 \tag{20}$$

and this should be compared to the line

$$Y = \left(1 - t_b - t_b^2 - t_b^3\right) g - t_b. \tag{21}$$

Since these lines are identical, the result is the pair of equations

$$2t_b^3 g_b^* = 1 - t_b - t_b^2 - t_b^3, \qquad t_b^3 [g_b^*]^2 = t_b. \tag{22}$$

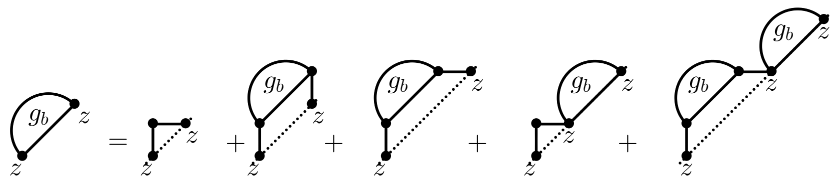

Figure 7. Every 1-bargraph path is either two edges as indicated above, or is a primitive 1-bargraph path with last edge vertical, or is a primitive 1-bargraph path with last edge horizontal, or is an arbitrary bargraph path preceded by two edges as shown, or is a primitive bargraph path with last edge horizontal and followed by an arbitrary bargraph path.

These equations can be solved simultaneously to give

$$t_b = \sqrt{2} - 1 \qquad \text{and} \qquad g_b^* = \sqrt{2} + 1. \tag{23}$$

The critical value of z can now be determined by considering equation (10). The radius of convergence of $g_{b,z}$ is given in equation (13), and the critical value of z is found by finding the infimum of z so that both $t = t_b$ and $tz(1 + t^2 z g_{b,1}) = 1$. Since $t = t_b$, this implies that $g_{b,1} = g_b^*$ in this, and thus

$$z_b = \inf_{z>0}\{z | tz(1 + t^2 z g_{b,1}) = 1, \text{ and } t = t_b, g_{b,1} = g_b^*\}. \tag{24}$$

Thus, z_b is the solution of

$$t_b z \left(1 + t_b^2 z g_b^*\right) = 1 \tag{25}$$

and solving this gives the result in equation (15).

The same calculations can be carried out for the model of paths with edge visits generated by ζ. Since t_b and g_b^* are already known, it only remains to consider the recurrence in equations (7) and (11). It follows that ζ_b is given by the solution of

$$\zeta\left(t_b + t_b^3 g_b^*\right) = 1. \tag{26}$$

Solving for ζ gives ζ_b in equation (16).

4. Bargraph paths in a 1-wedge

The q-wedge is defined as the wedge formed by the line $y = qX$ and the Y-axis. A bargraph path in a q-wedge is a partially directed path in the square lattice from the origin, confined to the q-wedge, and constrained to end in a vertex in the line $Y = qX$. A bargraph path in a 1-wedge is illustrated in figure 1(b). Vertices in the path that are on the line $Y = qX$ are *visits*, and observe that if $q > 0$, then it is not possible to have edge visits as in the model with recurrence $g_{b,\zeta}$ in equation (7). We call a bargraph path in a q-wedge a *q-bargraph path*.

One may directly enumerate q-bargraph paths, and the first few terms in the series are listed in table 1 for $q = 0, 1, \ldots, 5$. Observe that $q = 0$ corresponds to the usual model of bargraph paths with generating function g_b obtained in the previous sections. There are clear parity effects at work in table 1; if q is odd, then only even length paths are encountered, and even in the case that q is even the series appears to be initially somewhat uneven due to parity effects.

1-Bargraph paths can be enumerated by the scheme in figure 7. Define a *primitive* 1-bargraph path as a 1-bargraph path with its terminal (first and last) vertices in the line $Y = X$, but which is otherwise disjoint with this line. One may distinguish between primitive 1-bargraph paths with last edge vertical, or primitive 1-bargraph paths with last edge horizontal.

Table 1. Bargraph paths in q-wedges.

n	0-wedge	1-wedge	2-wedge	3-wedge	4-wedge	5-wedge
1	1					
2	1	1				
3	2		1			
4	4	3		1		
5	8		1		1	
6	16	10	3	1		1
7	33		1		1	
8	69	36	5	5		1
9	146		13		1	
10	312	137	7	7	5	1
11	673		28		1	
12	1 463	543	64	31	7	7
13	3 202		48		1	
14	7 050	2 219	165	53	9	9
15	15 605		346		36	
16	34 705	9 285	329	220	11	11
17	77 511		1 013		61	
18	173 779	39 587	1 998	432	13	64
19	390 966		2 273		91	
20	882 376	171 369	6 410	1 702	300	96
21	1 997 211		12 130		126	
22	4 532 593	751 236	15 823	3 702	587	133
23	10 311 720		41 537		166	
24	23 512 376	3328 218	76 574	13 967	979	681

Also observe that the shortest 1-bargraph path has length two edges: a vertical edge followed by a horizontal edge.

To find a recurrence relation for the generating function of 1-bargraph paths, consider figure 7. Argue now that each 1-bargraph path is either (1) the shortest 1-bargraph path of length two edges, or (2) is a primitive 1-bargraph path with last edge vertical, or (3) is a primitive 1-bargraph path with last edge horizontal, or (4) is composed of the shortest 1-bargraph path of length two edges, followed by an arbitrary 1-bargraph path or (5) finally is composed of a primitive 1-bargraph path with last edge horizontal, followed by an arbitrary 1-bargraph path. The resulting recurrence for the generating function $g_{1,z}$ is therefore

$$g_{1,z} = t^2z^2 + 2t^2z^2g_1 + t^2zg_{1,z} + t^2zg_1g_{1,z} \qquad (27)$$

where $g_1 = g_{1,1}$ is the generating function of 1-bargraphs with $z = 1$.

By putting $z = 1$ in equation (27), one obtains

$$t^2g_1^2 + (3t^2 - 1)g_1 + t^2 = 0 \qquad (28)$$

and this may be solved to find the generating function for 1-bargraphs:

$$g_1 = \frac{1 - 3t^2 - \sqrt{(1-t^2)(1-5t^2)}}{2t^2}. \qquad (29)$$

This can be verified by expanding and comparing coefficients with the data in table 1.

The radius of convergence can be determined to be $t_1^2 = 1/5$ and the value of the generating function at this point is $g_1^* = g_1(t_1) = 1$. Alternatively, one may follow the approach in section 3. In this event consider the pair of curves

$$Y = t^2g^2; \qquad Y = (1-3t^2)g - t^2, \qquad (30)$$

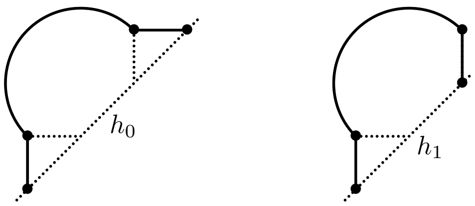

Figure 8. Bargraph paths in a q-wedge with last edge horizontal have generating function h_0, and bargraph paths in a q-wedge with last edge vertical are generated by h_1.

obtained from the recurrence in equation (28). Finding the tangent to $Y = t^2g^2$ at $(g_1^*, Y(g_1^*))$ and comparing it with the line $T = (1-3t^2)g - t^2$ at the critical point $(g_1^*, Y(g_1^*)$ again gives the values $t_1^2 = 1/5$ and $g_1^* = 1$. Finally, by considering the recurrence in equation (27), the solution for $g_{1,z}$ is

$$g_{1,z} = \frac{t^2z^2 + 2t^2z^2g_1}{1 - t^2z - t^2zg_1} \tag{31}$$

and the same arguments as in section 3 show that the critical value of z is the solution of

$$t_1^2z + t_1^2zg_1^* = 1. \tag{32}$$

This proves that

$$z_1 = 5/2. \tag{33}$$

5. Adsorbing bargraph paths in a q-wedge

5.1. The generating function

Finding the generating functions of q-bargraph paths is somewhat more involved than for the case of 1-bargaphs discussed above. In order to make progress, we define two generating functions: let h_0 be the generating function of q-bargraph paths with its final edge horizontal, and let h_1 be the generating function of q-bargraph paths with final edge vertically (down) oriented. These classes of q-bargraph paths are illustrated in figure 8. The first edge in each of the two classes is necessarily vertical, but the last edge determines the class. Observe that the class h_1 is terminal in the sense that the path cannot be continued from its last vertex. The full generating function of q-bargraphs is the sum of h_0 and h_1:

$$g_q = h_0 + h_1. \tag{34}$$

In the class of paths in h_0 there is a subclass of paths with exactly two visits to the adsorbing line $Y = qX$; these visits are necessarily the first and last vertices of the path. This class are the *primitive or prime* paths in h_0, and they will be denoted by $h_0^\dagger$. These paths can be constructed from the shortest q-bargraph path of length $q+1$ as illustrated in figure 9: Consider the lines $Y = qX + j$ for $j = 1, 2, \ldots, q$. Every path in the class $h_0^\dagger$ has a last vertex in $Y = qX + 1$, then a last vertex in $Y = qX + 2$ and so on until it has a last vertex in $Y = qX + q$. It must then return in one step to the line $Y = qX$.

Consider the last vertex v of the path in $Y = qX + j$ where $1 \leqslant j < q$. The vertex v is either the only vertex in this line, or it was preceded by a q-bargraph path from its first entry into the line. Since the last step in this path must be horizontal, this is generated by a factor $(1 + h_0)$, and the path continues from there by a vertical step to the next line. This pattern is only broken in the line $Y = qX + q$: in this case the path makes only one visit v to the line,

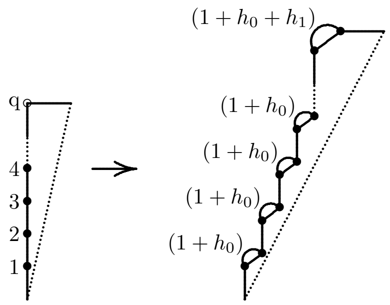

Figure 9. Primitive q-bargraph paths counted by the generating function h_0 can be constructed by taking the shortest q-bargraph path of length $p+1$, and then by observing that each of the vertices indicated by a • can be replaced by a vertex, or by a path generated by h_0. The exception is the vertex labelled by ○; it can be replaced either by an vertex, or by a path generated by either h_0 or h_1. Alternatively, one may instead note that each primitive q-bargraph path has a last vertex in the line $Y = qX + j$ for $j = 1, 2, \ldots, p$ and that it is a q-bargraph path generated by $1 + h_0$, or by $1 + h_0 + h_1$ at the last vertex in the line.

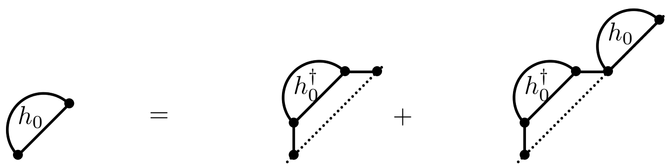

Figure 10. Every q-bargraph path counted by h_0 is either primitive, or it has a first return to the line $Y = qX$ followed by an arbitrary q-bargraph path counted by h_0. In this case it will be a primitive q-bargraph up to the first return.

or it is a q-bargraph path from the first visit to this line until its last visit. This is generated by a factor $(1 + g_q)$. The path is then followed by a horizontal step to the line $Y = qX$. In other words, the generating function of primitive paths in h_0 is given by

$$h_0^\dagger = t^{q+1}(1+h_0)^{q-1}(1+g_q) = t^{q+1}(1+h_0)^{q-1}(1+h_0+h_1). \tag{35}$$

Bargraph paths in the class h_0 can be decomposed into primitive paths in h_0 by a renewal argument: every path in h_0 is either a primitive path in h_0 or is composed of a primitive path followed by an arbitrary path in h_0 (see figure 10). In other words

$$h_0 = h_0^\dagger + h_0^\dagger h_0 = \frac{h_0^\dagger}{1 - h_0^\dagger}. \tag{36}$$

Next, consider the paths in the class h_1. These paths can be constructed by inserting two vertical edges in the end points of an arbitrary bargraph path, or by appending an arbitrary bargraph path with two vertical edges at its end point to a path in the class h_0. This is illustrated in figure 11, and the resulting relationship between h_1 and g_q is

$$h_1 = t^2 g_q + t^2 h_0 g_q = t^2(1+h_0)g_q. \tag{37}$$

In other words, one may express g_q in terms of h_0, using equation (37):

$$g_q = h_0 + h_1 = h_0 + t^2(1+h_0)g_q = \frac{h_0}{1 - t^2(1+h_0)}. \tag{38}$$

Observe that in turn

$$h_0 = \frac{(1-t^2)g_q}{1+t^2 g_q} \tag{39}$$

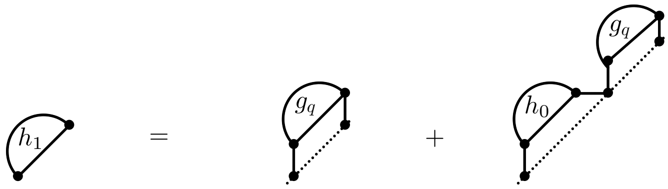

Figure 11. Every q-bargraph path counted by h_1 is in one of the two classes below: it is an arbitrary q-bargraph path translated one step in the Y-direction with two edges added to attach it to the line $Y = qX$, and a q-bargraph path in h_0 may be prepended to this.

and one may therefore solve for h_0 in equations (35) and (36) by noting that $g_q = h_0 + h_1$:

$$\begin{aligned} h_0 &= t^{q+1}(1+h_0)^q(1+g_q) \\ &= t^{q+1}(1+h_0)^q\left(1 + \frac{h_0}{1-t^2(1+h_0)}\right). \end{aligned} \tag{40}$$

In other words, h_0 is the root of a polynomial of degree $q+1$, and from it one may determine g_q by equation (38).

5.2. Critical values of t

Recurrences for the generating functions h_0 and g_q were determined above. These recurrences may be put into the form

$$h_0 = Th_0^2 + t^{q+1}(1+h_0)^{q+1}, \qquad \text{where} \quad T = \frac{t^2}{1-t^2}; \tag{41}$$

$$g_q = \frac{h_0}{1-t^2(1+h_0)}. \tag{42}$$

Consider the left- and right-hand sides of equation (41) separately: In particular, fix t and plot the functions

$$Y = h; \qquad Y = Th^2 + t^{q+1}(1+h)^{q+1} \tag{43}$$

on the same hY-plane. Intersections in the graphs of these functions will be solutions to equation (41). Observe that $Y = h$ is a straight line, while $Y = Th^2 + t^{q+1}(1+h)^{q+1}$ is convex for $h > 0$ and is also non-negative. There are at most two intersections between these curves, and the typical cases are illustrated in figure 12, where the curve $Y = f_q(h) = Th^2 + t^{q+1}(1+h)^{q+1}$ intersects the line $Y = h$ in two places and in one place respectively. Increasing t increases T and so the curvature and rate of increase in the curve in figure 12. Observe that as t increases, the solutions $h^{\pm}$ in figure 12(a) move together, and become one solution $h_0^* = h_0(t_q)$ at a critical value of $t = t_q$. For $t > t_q$ there are no intersections, and so no non-negative real solutions of equation (41). Thus, t_q is the critical value of t in the generating function h_0, and is its radius of convergence. Note that $h_0^* = h_0(t_q)$ is the value of h_0 when $t = t_q$, and that this is finite.

It follows from these arguments that one may determine both t_q and h_0^* by noting that the line $Y = h$ is tangent to the curve $Y = Th^2 + t^{q+1}(1+h)^{q+1}$ when $t = t_q$. The tangents to this curve at $h = h_0^*$ and $t = t_q$ are given by

$$Y = \left(2T_q h_0^* + (q+1)t_q^{q+1}(1+h_0^*)^q\right)h - T_q h_0^* + (1-qh_0^*)t_q^{q+1}(1+h_0^*)^q, \tag{44}$$

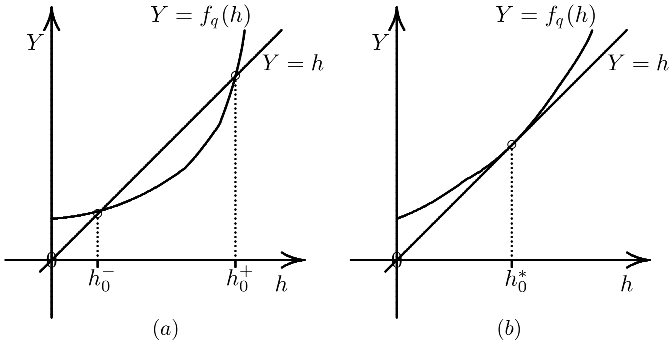

Figure 12. The functions in equation (43) plotted in the hY-plane. The function $Y = Th^2 + t^{q+1}(1+h)^{q+1}$ is convex for $h > 0$. For small values of t the situation is illustrated in (a). There are two points where the curves intersect; these give the non-negative solutions to equation (41). Increasing t leads to the situation in (b) where the line $Y = h$ is tangent to the function $Y = Th^2 + t^{q+1}(1+h)^{q+1}$ at a critical value of t, say when $t = t_q$. In this case the unique non-negative solution $h = h_0^*$ is the only non-negative solution of equation (41). If $t > t_q$, then there are no non-negative and real solutions.

where T_q is that value of T when $t = t_q$. This line should coincide with $Y = h$, and thus, t_q and h_0^* should be the solutions of

$$2T_q h_0^* + (q+1)t_q^{q+1}(1+h_0^*)^q = 1; \qquad -T_q[h_0^*]^2 + (1-qh_0^*)t_q^{q+1}(1+h_0^*)^q = 0. \tag{45}$$

From the second equation above it follows that

$$t_q^{q+1}(1+h_0^*)^q = \frac{T_q[h_0^*]^2}{1-qh_0^*}. \tag{46}$$

Substitute this factor into the first of the equations in (45) to obtain

$$2T_q h_0^* + (q+1)T_q\frac{[h_0^*]^2}{1-qh_0^*} = 1. \tag{47}$$

Thus, one may solve for T_q:

$$T_q = \frac{1-qh_0^*}{h_0^*(2+(1-q)h_0^*)} \tag{48}$$

and so also obtain an expression for t_q in terms of h_0^*. Substitute T_q and t_q into the second equation in (45) and simplify: this gives an expression for h_0^*:

$$(1+h_0^*)^q(1-qh_0^*)^{(q+1)/2}(2+(1-q)h_0^*) = h_0^*(1+(2-q)h_0^* + (1-q)[h_0^*]^2)^{(q+1)/2}. \tag{49}$$

This equation may be solved for h_0^*, and then T_q and t_q may be obtained from equation (48). This gives the radius of convergence of h_0, and the critical value of t for h_0. Comparison to the expression for g_q in equation (42) will then give information on the critical value of t for the generating function t_q and on $g_q^* = g_q(t_q)$.

5.3. *Example:* $q = 1$

Recall that h_0 is the generating function of bargraph paths as in figure 8(a), and that t_q is the radius of convergence of h_0. I have also defined $h_0^* = h_0(t_q)$, and this is finite. The function $T = t^2/(1-t^2)$ also has critical value T_q when $t = t_q$, and g_q is the full generating function of bargraph paths, and I also defined $g_q^* = g_q(t_q)$.

The relevant set of equations derived above are the following:

$$h_0^* = \frac{(1+h_0^*)^q(1-qh_0^*)^{(q+1)/2}(2+(1-q)h_0^*)}{(1+(2-q)h_0^*+(1-q)[h_0^*]^2)^{(q+1)/2}}, \tag{50}$$

$$T_q = \frac{1-qh_0^*}{h_0^*(2+(1-q)h_0^*)}, \tag{51}$$

$$t_q^2 = \frac{T_q}{1+T_q}, \tag{52}$$

$$g_q^* = \frac{h_0^*}{1-t_q^2(1+h_0^*)}, \tag{53}$$

as they were derived in equations (49), (48) and (42). Generally, one would proceed by solving for $h_0^* = h_0(t_q)$ in equation (50). This would give the critical values T_q and t_q^2, and finally one can determine $g_q^* = g_q(t_q)$. It is in particular important in this respect to make sure that the denominator in equation (53) does not vanish; that proves that the radius of convergence of h_0 is also the radius of convergence of g_q.

Consider for example the case $q = 1$; this model was solved in section 4. Putting $q = 1$ in equation (37) gives

$$3[h_0^*]^2 + h_0^* - 2 = 0. \tag{54}$$

Finding the roots of this quadratic gives $h_0^* = 2/3$ or $h_0^* = -1$, and since $h_0^* > 0$; the positive root is the sought solution. This produces $T_1 = 1/4$ and one obtains the critical value of t_1 derived in section 4: $t_1^2 = 1/5$. Finally, observe that the denominator in equation (53) is $1 - t_1^2(1+h_0^*) = 2/3 \neq 0$, and that $g_1^* = 1$.

5.4. The adsorption critical point

Consider now a model of bargraph paths in a q-wedge with a generating variable z counting visits in the line $Y = qX$. Increasing z will take this model through an adsorption transition at a critical value of $z = z_q$, and I showed in section 4 that $z_1 = 5/2$ for bargraph paths in a 1-wedge.

To determine z_q, first find recurrences for the generating functions of bargraph paths with z included as a generating variable. As before, let $h_0^\dagger$ be the generating function of primitive paths in h_0. Then by figure 10 and equation (36), the generating function $h_{0,z}$ of adsorbing paths in the class h_0 is given by

$$h_{0,z} = \frac{z^2 h_0^\dagger}{1 - z h_0^\dagger}. \tag{55}$$

This equation proves that the critical value of z in $h_{0,z}$ is determined by the condition that the above denominator vanishes.

One may also determine the generating function of adsorbing bargraph paths in the class h_1. Examining equation (37) and figure 11 gives the relation

$$h_{1,z} = t^2 z^2 g_{q,1} + t^2 z h_{0,z} g_{q,1} \tag{56}$$

for the generating function $h_{1,z}$ of bargraphs paths in the class h_1 with generating variable z for visits to the adsorbing line.

Since the generating function of adsorbing bargraph paths is given by the sum of $h_{0,z}$ and $h_{1,z}$, the above equations show that

$$g_{q,z} = h_{0,z} + t^2 z^2 g_{q,1} + t^2 z h_{0,z} g_{q,1}. \tag{57}$$

Table 2. Critical values for q-paths.

q	h_0^*	T_q	t_q^2	g_q^*	z_q
1	2/3	1/4	1/5	1	5/2
2	0.3937	0.3361	0.2516	0.6063	3.5399
3	0.2756	0.4341	0.3027	0.4489	4.6290
4	0.2113	0.5357	0.3488	0.3660	5.7317
5	0.1713	0.6380	0.3895	0.3149	6.8389
6	0.1439	0.7400	0.4253	0.2803	7.9475
7	0.1241	0.8414	0.4569	0.2552	9.0562
8	0.1091	0.9419	0.4850	0.2362	0.1016×10^1
9	0.9735×10^{-1}	0.1041×10^1	0.5101	0.2212	0.1127×10^2
10	0.8789×10^{-1}	0.1140×10^1	0.5327	0.2090	0.1238×10^2
15	0.5918×10^{-1}	0.1619×10^1	0.6182	0.1714	0.1790×10^2
20	0.4465×10^{-1}	0.2079×10^1	0.6752	0.1516	0.2339×10^2
50	0.1814×10^{-1}	0.4603×10^1	0.8215	0.1109	0.5611×10^2
10^2	0.9161×10^{-2}	0.8379×10^1	0.8934	0.9306×10^{-1}	0.11016×10^3
10^3	0.9379×10^{-3}	0.6230×10^2	0.9842	0.6305×10^{-1}	0.10672×10^4
10^4	0.9514×10^{-4}	0.4869×10^3	0.9980	0.4868×10^{-1}	0.10512×10^5
10^5	0.9602×10^{-5}	0.3983×10^4	0.9997	0.3977×10^{-1}	0.104142×10^6
10^6	0.9664×10^{-6}	0.3367×10^5	0.99997	0.3363×10^{-1}	0.1034805×10^7

In other words, if z_q is the critical value of z in $h_{0,z}$, then it is also the critical value of z in $g_{q,z}$. By equation (55) it follows that

$$z_q^{-1} = \sup_{0<t<t_q} \{h_0^\dagger\} \tag{58}$$

and if one consults equation (36), then

$$z_q = \inf_{0<t<t_q} \left\{ \frac{1+h_0}{h_0} \right\}. \tag{59}$$

Since h_0 increases with t, this infimum is realized when $t = t_q$ in which case $h_0 = h_0(t_q) = h_0^*$. Thus

$$z_q = \frac{1+h_0^*}{h_0^*}. \tag{60}$$

For example, if $q = 1$, then I computed that $h_0^* = 2/3$. Substitution gives $z_1 = 5/2$. This gives the value also computed in equation (33).

If $q > 1$, then the set of equations (50)–(53) cannot be solved explicitly, since h_0^* satisfies a polynomial of degree greater than 4. For example, if $q = 2$ then h_0^* satisfies a polynomial of degree 11. One may, however, approach the set of equations numerically and in table 2 the solutions are listed for a number of different values of q rounded to four decimal places.

6. Asymptotics for z_q

In equation (50) it was shown that h_0^* is a solution of the equation

$$h_0^* = (1+h_0^*)^q (2 + (1-q)h_0^*) \left(\frac{1 - q h_0^*}{1 + (2-q)h_0^* + (1-q)[h_0^*]^2} \right)^{(q+1)/2}. \tag{61}$$

Assume that that $h_0^* = u/q$, substitute this in the above and take the $1/q$th power. Then u is a solution of $f_q(u) = 0$, where

$$f_q(u) = \left(\frac{u}{q}\right)^{1/q} - \left(1+\frac{u}{q}\right)\left(2+\frac{(1-q)u}{q}\right)^{1/q}\left(\frac{1-u}{1+\frac{(2-q)u}{q}+\frac{(1-q)u^2}{q^2}}\right)^{(q+1)/2q}. \qquad (62)$$

An asymptotic expansion of $f_q(u)$ for large q can be determined using a symbolic computation program such as Maple [19]. This result is that

$$f_q(u) = \frac{1}{q}\left(\log u - \log q + \frac{u(u-2)}{2(u-1)} - \log(2-u) - u\right) + O\left(\frac{1}{q^2}\right). \qquad (63)$$

Assume that $u = 1 + U$. Assume that U is small and expand $f_q(u)$ in U to obtain

$$f_q(u) = \frac{1}{q}\left(\frac{3U}{2} - \frac{1}{2U} - 1 - \log q + O(U^2)\right). \qquad (64)$$

Since U is assumed to be small, ignore the $O(U^2)$ and higher order terms, and solve for $f_q(u) = 0$ to find U_0. The result is that

$$U_0 = \tfrac{1}{3}(1+\log q) - \tfrac{1}{3}\sqrt{\log^2 q + \log q^2 + 4}. \qquad (65)$$

For large q one may check that $U_0 \sim -1/\log q^2$, and so the assumption that U is small for large q is justified.

The function $u = 1 + U_0$ would be the solution of $f_q(u) = 0$ in equation (64) if the terms of order $O(U^2)$ are ignored (and if the terms of order $O(1/q^2)$ in equation (63) are ignored). To find the order of the error made by these assumptions, assume that $u = 1+U_0+\epsilon$ is the solution of $f_q(u) = 0$, where ϵ is an error term to be determined. Substitute this into equation (64) to observe that $\epsilon = O(1/|\log q|^2)$. In other words,

$$u = \frac{4}{3} + \frac{1}{3}\log q - \frac{1}{3}\sqrt{\log^2 q + \log q^2 + 4} + O\left(\frac{1}{|\log q|^2}\right). \qquad (66)$$

Thus, the following asymptotic expression should approximate h_0^*:

$$h_0^* = \frac{1}{3q}\left(4 + \log q - \sqrt{\log^2 q + \log q^2 + 4}\right) + O\left(\frac{1}{q|\log q|^2}\right). \qquad (67)$$

This result allows one to determine z_q by using equation (60):

$$z_q = \frac{3q + 4 + \log q - \sqrt{\log^2 q + \log q^2 + 4}}{4 + \log q - \sqrt{\log^2 q + \log q^2 + 4}} + O\left(\frac{q}{|\log q|^3}\right). \qquad (68)$$

This result immediately establishes that

$$\lim_{q\to\infty} \frac{z_q}{q} = 1. \qquad (69)$$

Since h_0^* is given asymptotically by equation (67), one may use it to determine values for T_q, t_q^2 and g_q^*. With increasing q, these asymptotic expressions are surprisingly accurate. For example, if $q = 50$ then $h_0^* \approx 0.0180$ and $z_{50} \approx 56.48$, and for $q = 100$, $h_0^* \approx 0.009\,13$ and $z_{100} \approx 110.55$. These values should be compared with the numerical estimates for z_q in table 2. With increasing q the asymptotic estimates become increasingly accurate, for example, one may check that the asymptotic estimates are $z_{1000} = 1067.65$, $z_{10\,000} = 10\,512.07$, $z_{100\,000} = 104\,142.62$ and $z_{1000\,000} = 1034\,805.50$. These numbers agree increasingly well with the results in table 2.

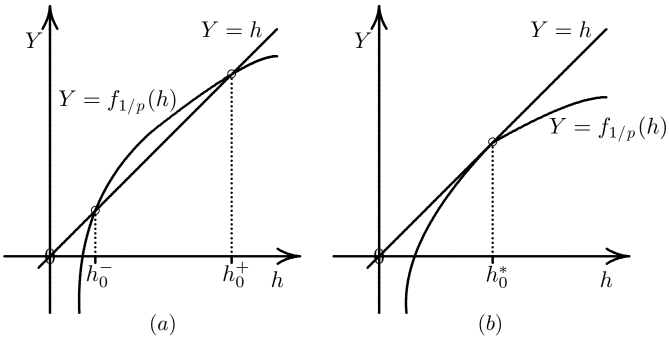

Figure 13. The curves in equation (74) plotted against $h \geqslant 0$. The curve $Y = \frac{1}{T} - \frac{t^{1+1/p}(1+h)}{T}(\frac{1+h}{h})^{1/p} = f_{1/p}(h)$ is concave for $h > 0$. The intersections are solutions of equation (73). For small values of t the solutions are real and the situation is illustrated in (a). Increasing t eventually gives rise to (b) at a critical value $t = t_{1/p}$ where there is one solution, and the line $Y = h$ is tangent to the curve $Y = \frac{1}{T} - \frac{t^{1+1/p}(1+h)}{T}(\frac{1+h}{h})^{1/p}$. For $t > t_{1/p}$ there are no real and non-negative solutions.

7. Bargraph paths in a $1/p$-wedge

In the previous sections, I considered bargraph paths adsorbing in a q-wedge, where q is a non-negative integer and the q-wedge is defined by the Y-axis and the line $Y = qX$. The above methods can be extended to a $1/p$-wedge where $p > 0$ is again an integer, and a $1/p$-wedge is formed by the line $Y = X/p$ and the Y-axis.

By applying the arguments developed in figure 9 to the path of length $p+1$ in a $1/p$-wedge, the generating function $h_p^\dagger$ of prime or primitive bargraph paths is given by

$$h_0^\dagger = t^{p+1}(1 + h_0 + h_1)^p, \tag{70}$$

where h_0 and h_1 are defined as in figure 8.

The remaining relations are as before: if $g_{1/p}$ is the generating function, then

$$g_{1/p} = h_0 + h_1, \qquad h_0 = \frac{h_0^\dagger}{1 - h_0^\dagger}, \qquad h_1 = t^2 g_{1/p}(1 + h_0). \tag{71}$$

These equations may be massaged to show that

$$g_{1/p} = \frac{h_0}{1 - t^2(1 + h_0)} \tag{72}$$

and h_0 is the solution of

$$h_0 = \frac{1}{T} - \frac{t^{1+1/p}(1 + h_0)}{T}\left(\frac{1 + h_0}{h_0}\right)^{1/p}, \tag{73}$$

where as before $T = t^2/(1 - t^2)$. One may again plot the left- and right-hand sides

$$Y = h; \qquad Y = \frac{1}{T} - \frac{t^{1+1/p}(1 + h)}{T}\left(\frac{1 + h}{h}\right)^{1/p} \tag{74}$$

of this equation against h to study its non-negative solutions. This is done in figure 13. For small values of t there are generally two non-negative solutions $h_0^\pm$, as shown in figure 13(a). Increasing t shows that there is a critical value $t_{1/p}$ of t where a unique non-negative solution

h_0^* is obtained. At this value of t, the line $Y = h$ is tangent to the curve given by the right-hand side of equation (73) at $h = h_0^*$.

The tangent at $h = h_0^*$ and $t = t_{1/p}$ of the curve in equation (74) is given by

$$Y = \left[\frac{t_{1/p}^{1+1/p}}{pT_{1/p}}\right]\left(\frac{1+h_0^*}{[h_0^*]^2}\right)^{1/p}(1 - p[h_0^*]^{1/p})(h - h_0^*) + \frac{1}{T_{1/p}} - \frac{t_{1/p}^{1+1/p}(1+h_0^*)}{T_{1/p}}\left(\frac{1+h_0^*}{h_0^*}\right)^{1/p},$$

where $T_{1/p} = t_{1/p}^2\big/\big(1 - t_{1/p}^2\big)$. Comparison to $Y = h$ at the critical point shows that $t_{1/p}$ and h_0^* should be solutions of the equations

$$\frac{t_{1/p}^{1+1/p}}{pT_{1/p}}\left(\frac{1+h_0^*}{[h_0^*]^2}\right)^{1/p}(1 - p[h_0^*]^{1/p}) = 1, \tag{75}$$

$$\frac{t_{1/p}^{1+1/p}(1+h_0^*)}{T_{1/p}}\left(\frac{1+h_0^*}{h_0^*}\right)^{1/p} = \frac{1}{T_{1/p}} - h_0^*. \tag{76}$$

Divide equation (76) by equation (75) to obtain

$$\frac{ph_0^*(1+h_0^*)}{1 - ph_0^*} = \frac{1}{T_{1/p}} - h_0^*. \tag{77}$$

This may be solved for $T_{1/p}$, $t_{1/p}^2$ and S:

$$T_{1/p} = \frac{1 - ph_0^*}{(1+p)h_0^*}, \qquad t_{1/p}^2 = \frac{1 - ph_0^*}{1 + h_0^*}, \qquad S = \left(\frac{1 - ph_0^*}{1 + h_0^*}\right)^{(p+1)/2p}. \tag{78}$$

These can be substituted into equation (75) and by simplifying,

$$(1 - ph_0^*)^{p+1} = \left(\frac{p}{1+p}\right)^{2p}[h_0^*]^2(1 + h_0^*)^{p-1}. \tag{79}$$

In other words, h_0^* is a root of a polynomial of degree $p+1$, and it should be the smallest positive root. One may verify that for $p = 1$ this reduces to $1 - h_0^* = h_0^*/2$ with solution $h_0^* = 2/3$; this is the value obtained in table 2.

The adsorbing model is obtained by inserting the generating variable z in the above analysis. In that case the full generating function is given by

$$g_{1/p,z} = h_{0,z} + h_{1,z} \tag{80}$$

where $h_{0,z}$ and $h_{1,z}$ are defined as before. One may again check that

$$h_{1,z} = \frac{h_{0,z}}{1 - t^2(1 + h_{0,z})} \tag{81}$$

and that $h_{0,z}$ satisfies the recurrence

$$h_{0,z} = \frac{z^2 h_0^\dagger}{1 - zh_0^\dagger}, \tag{82}$$

where $h_0^\dagger$ is the generating function of primitive or prime paths in h_0. This again shows that

$$z_{1/p}^{-1} = \sup_{0<t<t_{1/p}} \{h_0^\dagger\}, \tag{83}$$

similar to equation (58). In other words, by consulting equation (82) with $z = 1$ or equation (71), this shows that

$$z_{1/p} = \frac{1 + h_0^*}{h_0^*}, \tag{84}$$

Table 3. Critical values for $1/p$-paths.

p	h_0^*	$T_{1/p}$	$t_{1/p}^2$	$g_{1/p}^*$	$z_{1/p}$
1	2/3	1/4	1/5	1	5/2
2	0.3427	0.3060	0.2343	1/2	3.9181
3	0.2209	0.3817	0.2763	1/3	5.5270
4	0.1585	0.4616	0.3158	1/4	7.3079
5	0.1212	0.5421	0.3515	1/5	9.2524
6	0.9658×10^{-1}	0.6620	0.3835	1/6	1.1354×10^{1}
7	0.7931×10^{-1}	0.7011	0.4122	1/7	1.3609×10^{1}
8	0.6661×10^{-1}	0.7791	0.4379	1/8	1.6012×10^{1}
9	0.5695×10^{-1}	0.8561	0.4612	1/9	1.8561×10^{1}
10	0.4938×10^{-1}	0.9320	0.4824	1/10	2.5251×10^{1}
15	0.2797×10^{-1}	0.1297×10^{1}	0.5647	1/15	3.6753×10^{1}
20	0.1835×10^{-1}	0.1643×10^{1}	0.6216	1/20	5.5498×10^{1}
50	0.4386×10^{-2}	0.3491×10^{1}	0.7773	1/50	2.2902×10^{2}
10^2	0.1382×10^{-3}	0.6174×10^{1}	0.8606	10^{-2}	7.2459×10^{2}
10^3	0.2304×10^{-4}	0.4236×10^{1}	0.9769	10^{-3}	4.3404×10^{4}
10^4	0.3186×10^{-6}	0.3128×10^{2}	0.9968	10^{-4}	3.1386×10^{6}
10^5	0.4063×10^{-9}	0.2460×10^{3}	0.9996	10^{-5}	2.4610×10^{8}
10^6	0.4946×10^{-11}	0.2022×10^{4}	0.999 96	10^{-6}	2.0219×10^{10}

where $h_0^* = h_0(t_{1/p})$, similar to equation (60). By solving for h_0^* numerically, one may determine $t_{1/p}$, $g_{1/p}^* = g_{1/p}(t_{1/p})$ and $z_{1/p}$. The results are listed in table 3. Observe that $g_{1/p}^* = 1/p$ in this table.

An asymptotic estimate can also be found for $z_{1/p}$. Proceed by noting that h_0^* is a root of

$$\left(\frac{p}{p+1}\right)^2 h^{2/p}(1+h)^{1-1/p} - (1-ph)^{1+1/p} = 0. \tag{85}$$

Put $h = a/p$ and perform an asymptotic expansion of the left-hand side using Maple 9 [19]:

$$a + \frac{1}{p}(a + 2\log a - 2\log p - 2 - (1-a)\log(1-a)) + O\left(\frac{1}{p^2}\right) = 0. \tag{86}$$

Assume that $a \to 0^+$ as $p \to \infty$. Then the above term $(1-a)\log(1-a)$ can be ignored. Discard higher order terms and solve the resulting equation for a. This shows that

$$a = (p + O(1))\,\mathrm{e}^{1-W(ep(p+1)/2)}, \tag{87}$$

where $W(x)$ is the Lambert W-function. This gives an expression for h_0^*:

$$h_0^* = (1 + O(1/p))\,\mathrm{e}^{1-W(ep(p+1)/2)}. \tag{88}$$

The Lambert W-function has an asymptotic expression for large values of its argument:

$$W(x) \sim \log x - \log\log x + \frac{\log\log x}{\log x}, \tag{89}$$

see for example [18]. In other words,

$$h_0^* \approx (2 + O(1/p))\left[\frac{1+\log(p(p+1)/2)}{p(p+1)}\right]\exp\left(-\frac{\log(1+\log(p(p+1)/2))}{1+\log(p(p+1)/2)}\right). \tag{90}$$

One may substitute equation (90) into (84) to see that

$$z_{1/p} \approx 1 + (1 + O(1/p))\left[\frac{p(p+1)/2}{1+\log(p(p+1)/2)}\right]\exp\left(\frac{\log(1+\log(p(p+1)/2))}{1+\log(p(p+1)/2)}\right). \tag{91}$$

From this expression, or from equation (88), one may compute estimates of the critical value $z_{1/p}$ for large p. The results are adequate, but not of the same quality as for z_p given in equation (68). For example, if $p = 50$, then equation (88) estimates that $z_{1/50} \approx 203.10$ while equation (91) gives $z_{1/50} \approx 203.35$; the numerical solution in table 3 is $z_{1/50} = 229.0$. For $p = 1000$ the estimates are $z_{1/1000} = 42\,901.$ and $z_{1/1000} = 42\,746.$, and for $p = 1000\,000$, $z_{1/1000\,000} = 2.0218 \times 10^{10}$ and $z_{1/1000\,000} = 2.0162 \times 10^{10}$.

It appears that the asymptotic formula (91) approximates $z_{1/p}$ well for asymptotic values of p. Observe that

$$\lim_{p\to\infty} \frac{p^2 h_0^*}{\log p} = 4. \tag{92}$$

In the broadest terms, one may claim that $h_0^* \sim 4p^{-2}\log p$ with the result that

$$z_{1/p} \approx \frac{p^2}{2\log p^2} + 1 + o(1). \tag{93}$$

This approximation is not accurate for small values of p, but improves with increasing p. For example for $p = 100$ it is within 25% of the estimate in table 3, for $p = 10\,000$, within 14% and for $p = 1000\,000$, within 11%.

8. Conclusions

In this paper, solutions and approximations are presented for a model of bargraph paths in wedges formed by the Y-axis and the lines $Y = qX$ (q-wedges) or $Y = (1/p)X$ ($1/p$-wedges), where $p > 0$ and $q > 0$ are integers. A high quality estimate for the critical value of the visit generating variable z was obtained in q-wedges. However, while the approach to paths in $1/p$-wedges was successful, the problem appears to be more difficult in that case, and the estimates of the critical point were not accurate.

A similar study for Dyck paths in wedges produced the results $z_q = q + 1 = z_{1/q}$ for the critical values of the adsorption activity z. It appears much more difficult to find estimates of the critical value of z in q/p-wedges [14]. However, one may determine the entropic force the paths exert on the wedge explicitly [15]. In the model in this paper the results are more limited—this model is still not solved for bargraph paths in q- or $1/p$-wedges; we do not have solutions in closed form—only numerical solutions and asymptotic estimates are given above.

The most notable results are given in equations (68) and (91); these are approximate expressions for the critical adsorption activity for large p or q. In particular, it appears that

$$z_q \approx \frac{3q + 4 + \log q - \sqrt{\log^2 q + \log q^2 + 4}}{4 + \log q - \sqrt{\log^2 q + \log q^2 + 4}},$$

$$z_{1/p} \approx 1 + \left[\frac{p(p+1)/2}{1 + \log(p(p+1)/2)}\right] \exp\left(\frac{\log(1 + \log(p(p+1)/2))}{1 + \log(p(p+1)/2)}\right). \tag{94}$$

The expression for z_q proved much more accurate than the expression for $z_{1/p}$. Examination of the expression for $z_{1/p}$ shows that the exponential factor has a maximum at $p = 3$, that it approaches 1 as $p \to \infty$ and is bounded between 1 and 3/2 for all $p > 0$. In the large p case, it may be ignored, in which case only the ratio $p(p + 1)/2(1 + \log(p(p + 1)/2))$ survives; this gives the approximation in equation (93). It appears challenging to determine an expression for $z_{q/p}$ for a model of bargraph paths above the line $Y = (q/p)X$, but that remains an interesting and open problem.

Acknowledgment

EJJvR is supported by a grant from NSERC (Canada).

References

[1] Batchelor M T, Bennett-Wood D and Owczarek A L 1997 Two-dimensional polymer networks at a mixed boundary: surface and wedge exponents *J. Eur. Phys.* B **5** 139–42
[2] Brak R, Essam J M and Owczarek A L 1998 New results for directed vesicles and chains near an attractive wall *J. Stat. Phys.* **93** 155–93
[3] Brak R, Owczarek A L, Rechnitzer A and Whittington S G 2005 A directed walk model of a long polymer chain in a slit with attractive walls *J. Phys. A: Math. Gen.* **38** 4309–25
[4] Caracciolo S, Ferraro G and Pelissetto A 1991 Criticality of self-avoiding walks with an excluded infinite needle *J. Phys. A: Math. Gen.* **24** 3625–39
[5] Cardy J L and Redner S 1984 Conformal invariance and self-avoiding walks in restricted geometries *J. Phys. A: Math. Gen.* **17** L933–8
[6] Chayes J T and Chayes L 1986 Critical points and intermediate phases on wedges of Z^d *J. Phys. A: Math. Gen.* **19** 3033–48
[7] Colby S A, Gaunt D S, Torrie G M and Whittington S G 1987 Branched polymers attached in a wedge geometry *J. Phys. A: Math. Gen.* **20** L515–20
[8] de'Bell K and Lookman T 1985 Lattice trees and self-avoiding walks in a triangular lattice wedge *Phys. Lett.* A **112** 453–5
[9] Duplantier B and Saleur H 1986 Exact surface and wedge exponents for polymers in two dimensions *Phys. Rev. Lett.* **57** 3179–82
[10] Gaunt D S and Colby S A 1990 Branched polymers in a wedge geometry in three dimensions *J. Stat. Phys.* **58** 539–52
[11] Hammersley J M and Morton K W 1954 Poor man's Monte Carlo *J. R. Stat. Soc.* B **16** 23–38
[12] Hammersley J M and Whittington S G 1985 Self-avoiding walks in wedges *J. Phys. A: Math. Gen.* **18** 101–11
[13] Hara T and Slade G 1992 The lace expansion for self-avoiding walks in five or more dimensions *Rev. Math. Phys.* **4** 235–327
[14] Janse van Rensburg E J 2005 Square lattice directed paths adsorbing on the line $Y = qX$ *J. Stat. Mech.* in press
[15] Janse van Rensburg E J and Ye L 2005 Forces in square lattice directed paths in a wedge *J. Phys. A: Math. Gen.* **38** 8493–503
[16] Lawler G, Schramm O and Werner W 2004 On the scaling limit of planar self-avoiding walk *Proc. Conf. on Fractal Geometry and Applications: a Jubilee of Beniot Mandelbrot* vol 2 ed M Lapidus and M van Frankenhuijsen (Providence, RI: American Mathematical Society) pp 339–64
[17] Madras N N and Slade G 1993 *The Self-Avoiding Walk* (Boston, MA: Birkhäuser)
[18] http://mathworld.wolfram.com/LambertW-Function.html
[19] MAPLE 9 2004, Waterloo Maple Inc
[20] Prellberg T and Brak R 1995 Critical exponents from non-linear functional equations for partially directed cluster models *J. Stat. Phys.* **78** 701–30
[21] Prellberg T and Owczarek A L 1995 Stacking models of vesicles and compact clusters *J. Stat. Phys.* **80** 755–79
[22] Privman V, Forgacs G and Frisch H L 1988 New solvable model of polymer chains adsorbing on a surface *Phys. Rev.* B **37** 9897–900
[23] Vanderzande C 1998 *Lattice Models of Polymers Cambridge Lecture Notes in Physics* vol 11 (Cambridge: Cambridge University Press)
[24] Whittington S and Soteros C E 1990 Lattice animals: rigorous results and wild guesses *Disorder in Physical Systems* ed G Grimmett and D J A Welsh (Oxford: Oxford University Press) pp 323–35
[25] Wierman J C 1983 On square lattice directed percolation and resistance models *J. Phys. A: Math. Gen.* **16** 3545–51